Fast and simple fabrication of organic Bragg mirrors—application to plastic microchip lasers

2013 Laser Phys. Lett. 10 055808

(http://iopscience.iop.org/1612-202X/10/5/055808)

IOP PUBLISHING LASER PHYSICS LETTERS
Laser Phys. Lett. **10** (2013) 055808 (7pp) doi:10.1088/1612-2011/10/5/055808

LETTER

Fast and simple fabrication of organic Bragg mirrors—application to plastic microchip lasers

Leonid M Goldenberg, Victor Lisinetskii and Sigurd Schrader

University of Applied Sciences Wildau, Bahnhofstrasse, D-15745 Wildau, Germany

E-mail: goldenberg@th-wildau.de and lengold@gmx.de

Received 11 September 2012
Accepted for publication 11 February 2013
Published 10 April 2013
Online at stacks.iop.org/LPL/10/055808

Abstract
Organic Bragg mirrors with high reflectivity were fabricated on different substrates using a simple spin-coating procedure. Due to the simplicity of the procedure, the complete stack of layers could be fabricated within a very short time (approx. 30 min). Since one of the used polymers was based on azobenzene, it was possible to use photo-induced birefringence of the azobenzene material to tune the stop-band of the fabricated mirrors by means of illumination with polarized light. These Bragg mirrors were applied to fabricate microchip laser devices. Devices fabricated with different laser dyes exhibited conversion efficiencies of up to 4%.

(Some figures may appear in colour only in the online journal)

1. Introduction

Periodic modulation of the refractive index in one direction creates a photonic band gap or optical reflection in certain regions of the spectrum when the length scale of modulation is comparable to light wavelength [1]. These so-called one-dimensional photonic crystals have potential applications as antireflective coatings on lenses, colour pigments, interference filters and distributed Bragg reflectors or mirrors (DBR) in laser devices [1–3]. Well-established industrial procedures to fabricate highly reflective Bragg mirrors are vacuum evaporation, e.g. atomic layer deposition or sputtering of alternating layers of high and low refractive index materials, typically titania and magnesium fluoride [4]. The production of such interference mirrors is time consuming and expensive. A competitive approach would be based on the simple liquid phase deposition technique used in chemical laboratories, thus avoiding methods based on high vacuum. Such easy techniques have been pursued for the past few years. They are based on spin-coating of alternating multilayers of nanoparticles [2, 3, 5–9], sol–gel materials [10], hybrid organic–inorganic layers [11–15], and polymers [16–25]. Also co-extrusion of polymers has been reported [26, 27]. Such easily fabricated optical elements have several advantages. Commercially available polymers are usually very cheap. Nanoparticle suspensions, when produced on an industrial scale, should also be cheap. Polymer materials can be conveniently processed from solution or from the melt. Polymer processing techniques do not require high-vacuum equipment, which makes them comparably cost- and time-efficient. The fabrication can also be accomplished on different types of substrates (glass, plastic, elastic etc). On flexible or elastic substrates the properties of the mirrors can be tuned mechanically [22, 23, 28, 29] and also birefringence can be introduced [16]. Therefore, the fabrication of diffractive mirrors *via* spin-coating of commercially available polymers can be assumed to be an easy and cost-efficient fabrication method. In this process the properties are easily controlled by the concentration of the solution and the speed of rotation. A pair of polymers for the fabrication of mirror stacks are poly(*N*-vinylcarbazole) (PVC) and cellulose acetate (CA), with a refractive index difference of 0.2 [20–23].

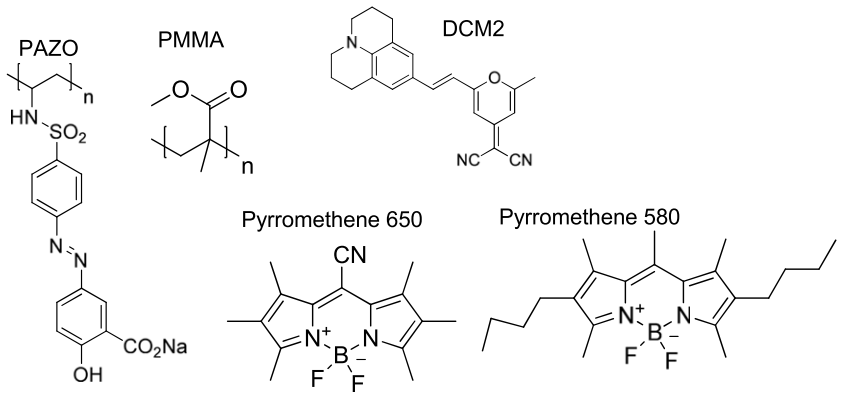

Figure 1. Chemical formulae of materials employed for fabrication of Bragg mirrors and DBR lasers.

High reflectivity has been obtained for a stack of 39 layers. However, the polymers used required a few minutes of baking after deposition of each layer. This complicates the process and renders it time consuming. In the search for an easier fabrication technique we have used our own results obtained with multi-stacks of surface relief gratings based on azobenzene-containing polyelectrolyte [30–32] and of the application of such stacks for bi-layer distributed feedback (DFB) lasers [33]. The pair of materials, which give a refractive index contrast of 0.28 and a good compatibility, is shown in figure 1 together with the used laser dyes.

Here we report an easy fabrication technique for highly reflective Bragg mirrors in a single continuous process without stopping the spin-coater. In this way a 35-layer mirror with a reflectivity of more than 90% is produced in approximately half an hour. We report here also the tuning of the polarized reflectivity of the mirror based on photo-induced birefringence of the azobenzene-containing material [34] and fabrication of a plastic microchip laser [35, 36] using such mirrors for the creation of a laser cavity.

2. Experimental details

Poly{1-[4-(3-carboxy-4-hydroxyphenylazo)benzenesulfonamido]-1,2-ethanediyl} (PAZO), polymethylmethacrylate, $M_w = 120\,000$ (PMMA) (both Aldrich), LD688 (DCM2), pyrromethene 580 and pyrromethene 650 laser dyes (all Exciton) have been used as received.

Multilayers were produced on glass or plastic (PE) substrates from a solution of PAZO in methanol (20.2 g l^{-1}) and PMMA in toluene (30.9 g l^{-1}) using a SCE-150 spin-coater (Lot-Oriel) at a rotation speed of 75 rps. The first and the last layer were always made of PAZO. An active light generating layer was cast from a 1% solution of the selected laser dye in PMMA in toluene or chlorobenzene. A back-reflection aluminum mirror was evaporated afterwards in vacuum.

The thickness was measured using a Veeco Dektak 150 profilometer. UV–vis spectra in both transmission and specular reflection geometries (angle 20°) were measured using a Specord M42 spectrometer (Carl-Zeiss Jena). An aluminum mirror was used as a standard in reflection measurements. Birefringence was induced by exposure of the stack to the light of an Ar^+ laser (Spectra Physics) operating at 488 nm. A *Q*-switched frequency doubled Nd:YAG pulsed laser (Surelite I, Continuum, Inc.) operating at 532 nm with a pulse duration of 6 ns and repetition rate of 10 Hz was used as the pump source for investigation of the DBR laser. The output signal was collected by an optical fibre, which was coupled to a CCD-based spectrometer (Polytec Berlin AG) with a spectral resolution of about 1.5 nm. The energy of the pump and of output pulses was measured with an energy meter LEM2020 (Sensor- und Lasertechnik, Germany) connected to a pyroelectric head PEM 4.

3. Results

It was previously established [30–33] that multilayer stacks could be prepared from the polar azobenzene-containing polyelectrolyte PAZO with a high refractive index of $n = 1.67$ [33] and of the non-polar, low refractive index polymer PMMA with $n = 1.49$, or even with the higher refractive index PPQ with $n = 1.75$ [33]. In these studies [30–33] we have used 2-methoxyethanol as the solvent for spin-coating of PAZO to yield very smooth films [30, 31]. However, 2-methoxyethanol is a relatively high boiling solvent (b.p. 120 °C), and consequently similarly to the polymer pair PVC-CA [20–23], a deposition from this solvent would require baking after each stage to remove the rest of the solvent. To avoid the baking step we have used low boiling point methanol (b.p. 65 °C), as originally used for the fabrication of PAZO holographic layers [34]. This allows continuous alternating deposition of the pair of polymers (PAZO from methanol and PMMA from toluene) without stopping the rotation and the appearance of reflection from the interference mirror could be observed on the spin-coater (figure 2(a)).

The parameters of multilayer structures were calculated using the method described in [37]. In this method a stack matrix for the structure is calculated as follows:

$$\mathbf{S} = \begin{pmatrix} S_{11} & S_{12} \\ S_{21} & S_{22} \end{pmatrix} = \mathbf{T_{N(N+1)}P_NT_{(N-1)N}P_{N-1}}\cdots\mathbf{T_{12}P_1T_{01}}, \quad (1)$$

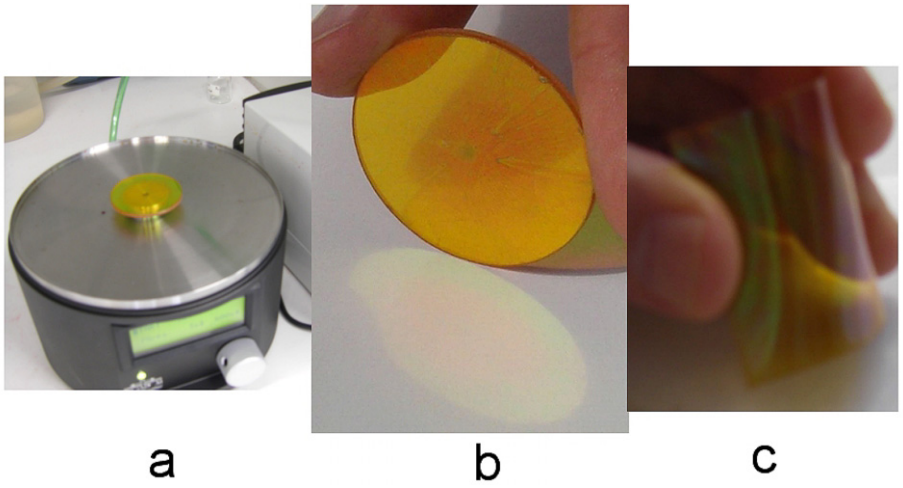

Figure 2. Photographs of interference mirror samples: (a) on the spin-coater chuck; (b) showing reflection colours; (c) showing reflection colours after bending on a plastic substrate.

where $\mathbf{P_j}$ is a propagation matrix, describing the phase shift introduced during propagation through the jth layer with thickness L_j and refractive index n_j:

$$\mathbf{P_j} = \begin{pmatrix} \exp\left(\mathrm{i}\frac{2\pi}{\lambda} n_j L_j\right) & 0 \\ 0 & \exp\left(-\mathrm{i}\frac{2\pi}{\lambda} n_j L_j\right) \end{pmatrix}. \quad (2)$$

$\mathbf{T_{ij}}$ is the transition matrix connecting the electric field amplitudes on both sides of the interface between the ith and jth layers:

$$\mathbf{T_{ij}} = \frac{1}{\sqrt{1 - r_{ij}^2}} \begin{pmatrix} 1 & -r_{ij} \\ -r_{ij} & 1 \end{pmatrix}, \quad (3)$$

where r_{ij} is the amplitude reflection coefficient for a transition from the ith layer to the jth layer:

$$r_{ij} = \frac{n_i - n_j}{n_i + n_j}. \quad (4)$$

The zeroth layer in equation (1) is a glass substrate, while the $(N+1)$th layer is air. No absorption was assumed in the layers.

Finally, the reflectivity of the multilayer structure can be calculated using the stack matrix $\mathbf{S}$ as follows:

$$R = \left|\frac{S_{12}}{S_{22}}\right|^2. \quad (5)$$

Calculations were performed for a refractive index of PAZO equal to 1.67 [33], PMMA equal to 1.49 [2], and the glass substrate equal to 1.5.

Usually in multilayer mirrors [37] the optical thickness of each layer is equal to a quarter wavelength multiplied by an odd integer. However, our calculations showed that it is enough to control the optical thickness of a bi-layer. Figure 3 shows the mirror reflectivity calculated for 35 layers for two cases: in the first case (solid line) the geometrical thickness of each layer was equal to 101.9 nm. The optical thicknesses of the PAZO and PMMA layers were about

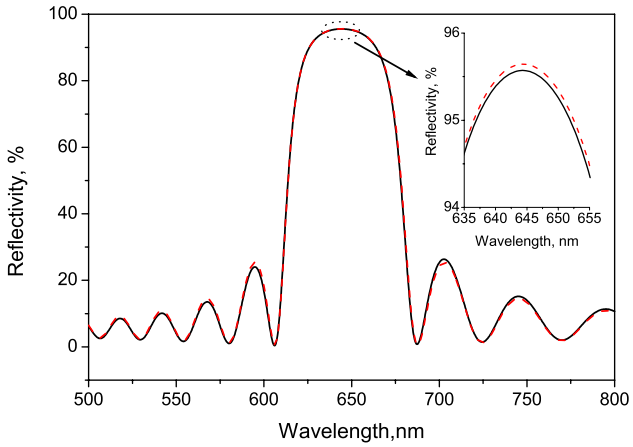

Figure 3. Reflectivity of a 35-layer mirror versus wavelength. The solid line corresponds to the case of different thicknesses of the PAZO- and the PMMA layers. The dashed line is for the case where the thicknesses of the PAZO- and the PMMA layers are equal.

170.1 nm and 151.8 nm, respectively. The optical thickness of the bi-layer was about 322 nm, which corresponds to half of the wavelength of minimum reflectivity (644 nm). In the second case (dashed line) the optical lengths of each layer were equal to 161 nm (the quarter of 644 nm). It can be seen that the difference between these two cases is negligible. So, we can produce multilayer structures by ensuring that the optical thickness of a bi-layer is equal to half of the required wavelength.

In preparation of the multilayer mirror the control of layer thickness was performed by adjusting the polymer solution concentration and rotation speed. The thickness of each layer was nearly equal to 100 nm (measured by profilometer). The optical thickness of the PAZO layers was about 170 nm and that of the PMMA layers was about 150 nm. Hence, the optical length of a bi-layer was about 320 nm, which causes a spectral stop-band around 640 nm. In this way multilayer stacks can be deposited on glass or plastic

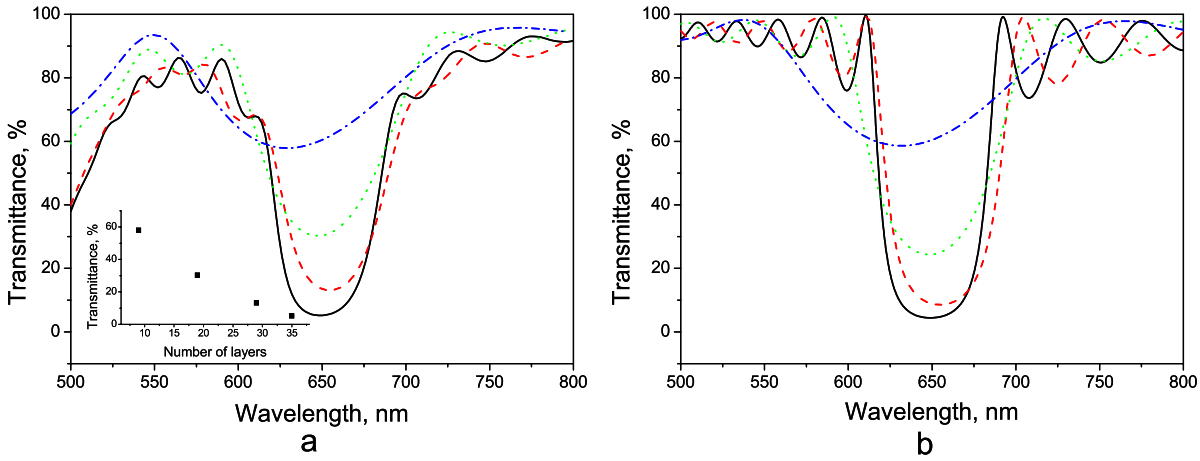

Figure 4. Spectra of multilayer mirrors (a) measured (the inset shows the dependence of the transmittance minimum on the number of layers) and (b) calculated spectra (for details see text).

substrates. Figure 4(a) presents the transmittance spectra measured for 9-, 19-, 29-, and 35-layer mirrors spin-coated on a glass plate. It can be seen that even a 9-layer mirror exhibits a stop-band, and the depth of the stop-band increases with the number of layers (see the inset in figure 4(a)). Unfortunately, we could not realize a high reproducibility of the bi-layer thickness. The thickness was slightly different in different multilayer structures. This resulted in a certain wavelength shift of the stop-band (figure 4(a)). Using the stop-band position shown in figure 4(a) we can estimate that the bi-layer optical thickness was equal to 315 nm for the 9-layer structure, 324 nm for the 19-layer structure, 327 nm for the 29-layer structure, and 325 nm for the 35-layer structure. The transmittance of the multilayer mirrors calculated for these values of bi-layer thickness is presented in figure 4(b). The geometrical thickness of all layers in a multilayer structure was assumed to be constant. The good correspondence between experimental and calculated dependences is evident. The difference between experimental and calculated curves, especially in the spectral region 500–550 nm, can be explained by the absorption of PAZO. Our calculation did not consider this absorption. In the middle of the mirror stop-band (near 650 nm) PAZO absorption is small and both the experimental and calculated transmittance spectra show a transmittance minimum of the 35-layer mirror equal to 5%. The reflectivity of this mirror was experimentally compared with a commercial Al-mirror (reflectivity at a wavelength of 650 nm is about 92%) at an incidence angle of 20°. The comparison shows that the reflectivity of our 35-layer mirror is even slightly higher than 92%. This means that the absorbance of the mirror in the specified spectral region is very small (1–2 % or less).

As can be seen in figure 4(a), the spectra of the mirrors, especially of the 35-layer mirror, show characteristic Fabry–Perot fringes. Similarly to three-dimensional colloidal crystals [38] such an observation indicates the high quality of the one-dimensional photonic crystal and allows the calculation of the total multilayer thickness. The values of thickness measured by means of profilometer, calculated by using the position of the Fabry–Perot fringes, and from the simulation were similar.

The suggested method of preparation of the multilayer structure can be employed for fabrication of organic lasing devices. Two device configurations can be envisaged. The first configuration is a DFB laser, which has already been realized with other multilayer structures fabricated by spin-coating [2, 3, 15, 20, 22]. In the reported design each second layer in the multilayer architecture contains an emitter [15, 20, 22]. The second lasing device configuration is a DBR laser, where the multilayer structure works as one of the mirrors in the laser cavity. Such a device was realized using sol–gel multilayer structures and the emitter in liquid crystal matrix [10] and mixed for a TiO_2 nanoparticles–PMMA multilayer [2]. The second configuration has the advantage that many different polymer matrices can be used as an active layer depending on which layer (polar polymer or non-polar polymer) is the last one in the multilayer structure. This allows the use of a variety of laser dyes or other emitting materials, the variation of their concentration and the optimization of the thickness of the active layer. In contrast, for the DFB laser structure the laser dye can in our case only be introduced into the PMMA layer, as azobenzene usually quenches luminescence [33, 39], and because the majority of laser dyes are of a polar nature not many of them could be introduced into PMMA-toluene solution in high concentration. Naturally, for other systems with DFB structure, the emitter can be introduced into either the polar or the non-polar layer, and the polar CA layer has already been used for the introduction of the laser dye Rhodamine 6G [20, 22].

In this letter we demonstrate that the previously discussed organic Bragg mirror can be used as the output coupler in an organic microchip laser [35, 36]. Microchip lasers were realized by coating the above discussed organic Bragg mirrors with gain layers of PMMA doped with dyes such as pyrromethene 580, pyrromethene 650 or LD688. The rare mirror was made by deposition of an aluminum layer onto the gain layer in vacuum (figures 5(a) and (b)). The DBR lasers were pumped through the Bragg mirror at an incidence angle

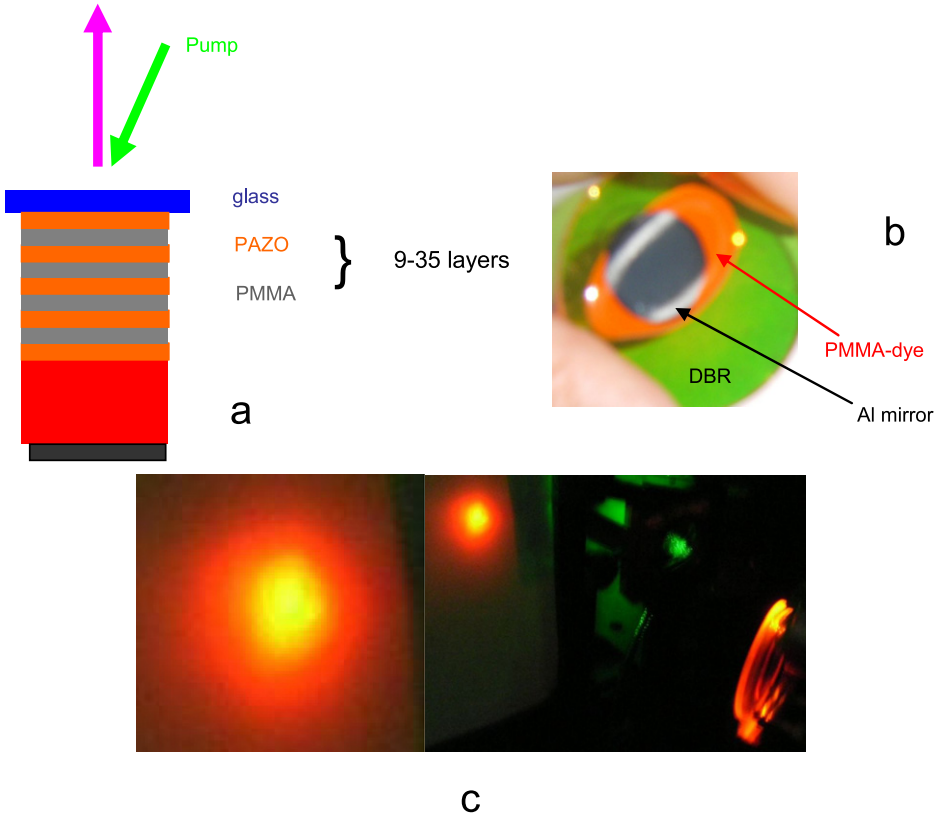

Figure 5. (a) Scheme of the DBR laser, (b) photograph of a fabricated DBR laser, (c) photographs of a working laser: 35-layer DBR mirror with the gain medium PMMA doped with 1% by weight of LD688, 350 μm thick.

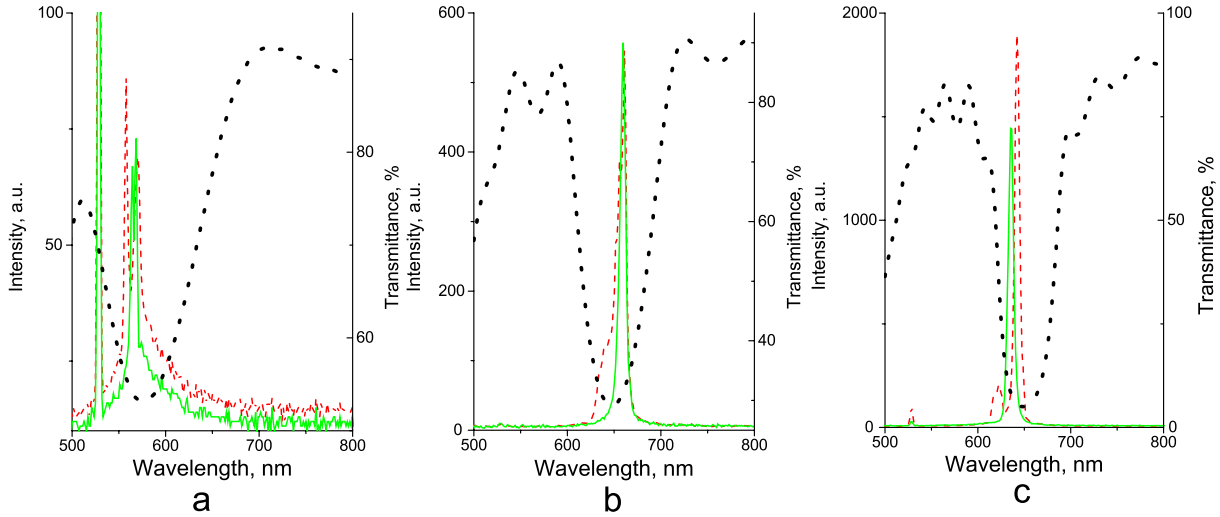

Figure 6. Spectra of laser generation together with the stop-band (dashed line) for DBR lasers: (a) DBR of 9-layers with pyrromethene 580 in the PMMA matrix (0.5% by weight, gain layer thickness 77 μm); (b) DBR of 19 layers with pyrromethene 650 in the PMMA matrix (0.5% by weight, gain layer thickness 60 μm); (c) DBR of 35 layers with LD688 in the PMMA matrix (1 % by weight, gain layer thickness 350 μm); red and green lines correspond to different measurements, each of which was carried out by averaging over 100 pulses.

of about 30° as illustrated in figure 5(a). The pump beam diameter was about 0.8 mm.

Already the Bragg mirror with 9 layers shows sufficient reflected power to yield laser generation (figure 6(a)). Several examples of lasing spectra for active media with different laser dyes generating at different wavelengths (DBR with different number of layers) are presented in figure 6. It is evident that for all cases laser generation was reached. It was found that the generation wavelength changes with time. Sometimes several wavelengths were generated simultaneously (see figure 6(a)). This behaviour can be explained by the competition of longitudinal modes of the cavity.

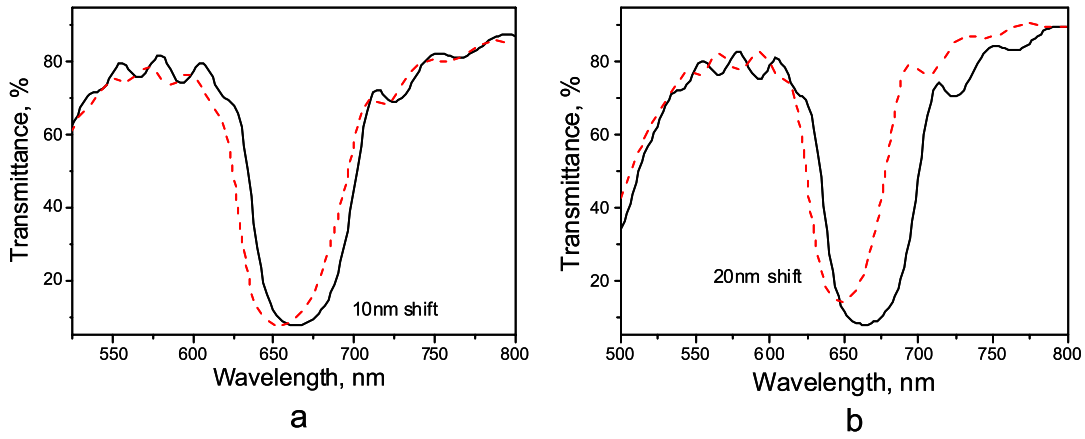

Figure 7. Changes in transmittance spectra of a 35-layer Bragg mirror after exposure to vertically polarized 488 nm light: solid lines are spectra before exposure; dashed lines are spectra after exposure, registered: (a) with non-polarized, (b) with vertically polarized light.

Certainly the reflective power of the DBR determined by the number of layers strongly influences the laser device performance. While for the laser with 35 layers DBR shown at figure 6(c) a lasing threshold of 8 mJ cm^{-2} has been observed, for the lasing devices with lower numbers of layers (consequently with lower reflection, spectra at figures 6(a) and (b)) the lasing threshold was at least 10 times higher. The generated beam for the best performing laser is presented in figure 5(c). Good central symmetry of the beam is evident. The beam divergence was about 200 mrad. Conversion efficiency has been measured to be about 4%. Direct comparison with other reported laser devices based on a multilayer architecture prepared by spin-coating would be difficult, while not all data were reported and different device configurations, emitters, dye concentration and active length were used. Just to mention, a polymer DFB structure [22] and polymer-nanoparticles DBR structure [2] exhibited a higher lasing threshold of 17 mJ cm^{-2}, while DFB structures where the emitter has been absorbed into a sintered mirror [3], and where one of the layers in a multilayer structure was the layer of a light emitting polymer [15], exhibited much lower threshold below 1 mJ cm^{-2}.

The peculiarity of materials used in the preparation of the DBR is that the azobenzene-containing polyelectrolyte PAZO, as many other side-chain azobenzene polymers, could be oriented by linearly polarized light [34]. In this way we were able to produce an optically responsive one-dimensional photonic crystal (see figure 7). Here the transmittance minimum (position of the stop-band) can be shifted by 10–20 nm when optical birefringence is photo-induced in the PAZO layers of the multilayer structure. The effect can be used for tuning other optical properties dependent on the position of the stop-band. Potential applications of other azobenzene-containing materials exhibiting higher photo-induced birefringence (e.g. liquid crystalline materials) may further increase the optical tunability of the DBR mirror. For example, a comparison of the area exposed to linearly polarized light with an unexposed area of a plastic microchip laser exhibits the trend that the photooriented area which shows a hypsochromic shift of the stop-band in the spectrum (figure 7), generates light at a shorter wavelength (figure 8). Tuning over 10 nm was achieved. However, more detailed investigations of optical tuning of the laser generation wavelength will be performed within further studies.

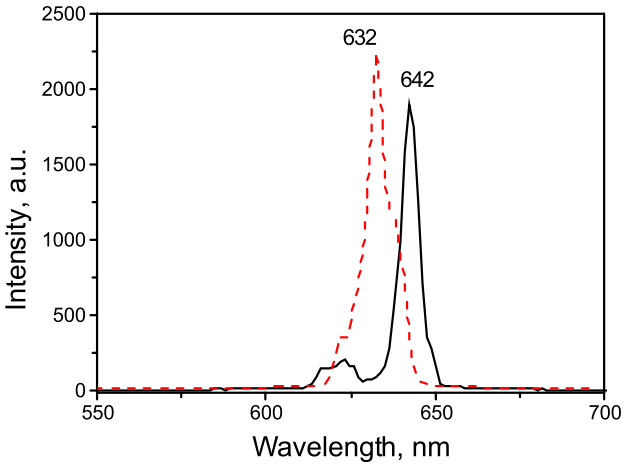

Figure 8. Spectra of laser generation in a 35-layer DBR laser device with LD688 in the PMMA matrix (1% by weight, gain layer thickness 190 μm), where the DBR was not exposed (solid line) and exposed (dashed line) to vertically polarized light of 488 nm prior to the lasing experiment.

4. Conclusions

Multilayer Bragg reflective mirrors were fabricated by a fast and simple continuous procedure, which is essentially an alternating spin-coating of two different polymer solutions. Because one of the polymers was a side-chain azobenzene-containing polymer, birefringence could be introduced into these layers by exposing them to linearly polarized light at 488 nm. In this way the stop-band of the Bragg mirror can be optically tuned. Using such fabricated DBR mirrors, the creation of laser cavity devices with different laser dyes and different numbers of layers has been achieved. The best devices exhibited light conversion efficiencies up to 4%.

Acknowledgments

The authors would like to thank Dr V Ksianzou (University of Applied Sciences Wildau) for aluminum vacuum deposition.

References

[1] Ge J and Yin Y 2011 *Angew. Chem. Int. Edn* **50** 1492
[2] Yoon J, Lee W, Caruge J-M, Bawendi M, Thomas E L, Kooi S and Prasad P N 2006 *Appl. Phys. Lett.* **88** 091102
[3] Scotognella F, Puzzo D P, Monguzzi A, Wiersma D S, Maschke D, Tubino R and Ozin G A 2009 *Small* **5** 2048
[4] Paschotta R 2009 *Bragg Mirrors* (*Encyclopedia of Laser Physics and Technology*) RP Photonics www.rp-photonics.com/encyclopedia.html
[5] Calvo M E and Miguez H 2010 *Chem. Mater.* **22** 3909
[6] Sanchez-Sobrado O, Calvo M E and Miguez H 2010 *J. Mater. Chem.* **20** 8240
[7] Redel E, Huai C, Renner M, von Freymann G and Ozin G A 2011 *Small* **7** 3465
[8] Bonifacio L D, Lotsch B V, Puzzo D P, Scotognella F and Ozin G A 2009 *Adv. Mater.* **21** 1641
[9] Kurt P, Banerjee D, Cohen R E and Rubner M F 2009 *J. Mater. Chem.* **19** 8920
[10] Lee S H and Ha N Y 2011 *Small* **7** 2704
[11] Guldin S, Kolle M, Stefik M, Langford R, Eder D, Wiesner U and Steiner U 2011 *Adv. Mater.* **23** 3664
[12] Wang Z *et al* 2012 *ACS Appl. Mater. Interfaces* **4** 1397
[13] Schneider D, Liaqat F, El Boudouti E H, Hassouani Y El, Djafari-Rouhani B, Tremel W, Butt H-J and Fytas G 2012 *Nano Lett.* **12** 3101
[14] Gomopoulos N, Maschke D, Koh C Y, Thomas E L, Tremel W, Butt H-J and Fytas G 2010 *Nano Lett.* **10** 980
[15] Puzzo D P, Scotognella F, Zavelani-Rossi M, Sebastian M, Lough A J, Manners I, Lanzani G, Tubino R and Ozin G A 2009 *Nano Lett.* **9** 4273
[16] Weber M F, Stover C A, Gilbert L R, Nevitt T J and Ouderkirk A J 2000 *Science* **287** 2451
[17] Katouf R, Komikado T, Itoh M, Yatagai T and Umegaki S 2005 *Photon. Nanostruct.* **3** 116
[18] Mönch W, Dehnert J, Jaufmann E and Zappe H 2006 *Appl. Phys. Lett.* **89** 164104
[19] Mönch W, Dehnert J, Prucker O, Rühe J and Zappe H 2006 *Appl. Opt.* **45** 4284
[20] Komikado T, Yoshida S and Umegaki S 2006 *Appl. Phys. Lett.* **89** 061123
[21] Komikado T, Inoue A, Masuda K, Ando T and Umegaki S 2007 *Thin Solid Films* **515** 3887
[22] Scotognella F, Monguzzi A, Meinardi F and Tubino R 2010 *Phys. Chem. Chem. Phys.* **12** 337
[23] Inoue A, Komikado T, Kinoshita K, Hayashi J and Umegaki S 2007 *Japan. J. Appl. Phys.* **46** L1016
[24] Frezza L, Patrini M, Liscidini M and Comoretto D 2011 *J. Phys. Chem.* C **115** 19939
[25] Wang Z *et al* 2012 *J. Mater. Chem.* **22** 7887
[26] Singer K D, Kazmierczak T, Lott J, Song H, Wu Y, Andrews J, Baer E, Hiltner A and Weder C 2008 *Opt. Express* **16** 10358
[27] Kazmierczak T, Song H, Hiltner A and Baer E 2007 *Macromol. Rapid Commun.* **28** 2210
[28] Kolle M, Zheng B, Gibbons N, Baumberg J J and Steiner U 2010 *Opt. Express* **18** 4356
[29] Kamita G, Kolle M, Huang F, Baumberg J J and Steiner U 2012 *Opt. Express* **20** 6421
[30] Goldenberg L M, Gritsai Y, Kulikovska O and Stumpe J 2008 *Opt. Lett.* **33** 1309
[31] Gritsai Y, Goldenberg L M, Kulikovska O and Stumpe J 2008 *J. Opt.* A **10** 125304
[32] Gritsai Y, Goldenberg L M, Kulikovska O, Sakhno O and Stumpe J 2010 *Proc. SPIE* **7716** 77161V
[33] Goldenberg L M, Lisinetskii V, Gritsai Y, Stumpe J and Schrader S 2012 *Opt. Mater. Expr.* **2** 1597
[34] Goldenberg L M, Kulikovska O and Stumpe J 2005 *Langmuir* **21** 4794
[35] Zayhowski J J 1999 *Opt. Mater.* **11** 255
[36] Molva E 1999 *Opt. Mater.* **11** 289
[37] Hodgson N and Weber H 2005 *Laser Resonators and Beam Propagation. Fundamentals, Advanced Concepts and Applications* 2nd edn (New York: Springer) p 653
[38] Jiang P, Bertone J F, Hwang K S and Colvin V L 1999 *Chem. Mater.* **11** 2132
[39] Goldenberg L M, Lisinetskii V, Gritsai Y, Stumpe J and Schrader S 2012 *Adv. Mater.* **24** 3339